Proof of region-specific multipotent progenitors in human breast epithelia

Agla J. Fridriksdottir[a,b,1], René Villadsen[a,b,1], Mikkel Morsing[a,b], Marie Christine Klitgaard[a,b,c], Jiyoung Kim[a,b], Ole William Petersen[a,b], and Lone Rønnov-Jessen[c,2]

[a]Department of Cellular and Molecular Medicine, Faculty of Health Sciences, University of Copenhagen, DK-2200 Copenhagen N, Denmark; [b]Novo Nordisk Foundation Center for Stem Cell Biology, DanStem, Faculty of Health Sciences, University of Copenhagen, DK-2200 Copenhagen N, Denmark; and [c]Section for Cell Biology and Physiology, Department of Biology, Faculty of Science, University of Copenhagen, DK-2100 Copenhagen Ø, Denmark

Edited by Zena Werb, University of California, San Francisco, CA, and approved October 9, 2017 (received for review August 16, 2017)

The human breast parenchyma consists of collecting ducts and terminal duct lobular units (TDLUs). The TDLU is the site of origin of most breast cancers. The reason for such focal susceptibility to cancer remains poorly understood. Here, we take advantage of a region-specific heterogeneity in luminal progenitors to interrogate the differentiation repertoire of candidate stem cells in TDLUs. We show that stem-like activity in serial passage culture and in vivo breast morphogenesis relies on the preservation of a myoepithelial phenotype. By enrichment for region-specific progenitors, we identify bipotent and multipotent progenitors in ducts and TDLUs, respectively. We propose that focal breast cancer susceptibility, at least in part, originates from region-specific myoepithelial progenitors.

breast | myoepithelial cell | stem cell | progenitors

It is increasingly appreciated that the site of origin of cancer at the histological level impacts severely on the tumor phenotype and the course of disease (1). The human breast consists of ducts which end in facultative secretory units referred to as terminal duct lobular units (TDLUs). The permanent presence of relatively well-developed, albeit resting, TDLUs under nonlactating conditions is a hallmark of the human breast (2, 3). This seems to be highly relevant from a cancer perspective because, presumably, around three-fourths of all human breast cancers arise specifically in TDLUs (1). Indeed, both the mammographic and histological presentations and clinical outcomes are entirely different between TDLU- and duct-derived breast cancers (1). Hence, given the rising appreciation of predecessor cells as impacting on tumor phenotypes, it is tempting to speculate that TDLUs and ducts rely on different cells for maintenance of tissue homeostasis and, in turn, tumor initiation. Indeed, our previous studies suggest that the anatomical location of a stem cell zone may be of relevance for the characteristics of the generated progenitors of luminal cells (4). Here, we decided to take advantage of early observations that TDLUs and ducts differ by cytokeratin 19 (K19) expression (5). The TDLUs are often heterogeneous, while the ducts consistently are homogeneously $K19^+$. Moreover, the likely TDLU-derived benign breast lesions are also heterogeneous, while the duct-derived papillomas are homogeneously $K19^+$ (5). These differences were all found within the luminal epithelial lineage. More recently, it has been overwhelmingly demonstrated that the luminal epithelial lineage originates from stem cells residing within the myoepithelial lineage (6–8). Moreover, alteration of the PI3K signaling pathway in mice leads to destabilization of the myoepithelial lineage and generation of luminal tumors (9). Therefore, to examine the cellular source of heterogeneity within the luminal lineage, measures to address progenitor cells within the myoepithelial lineage are highly warranted.

All attempts so far to measure human breast progenitor cell activity have suffered from lack of control of lineage, as well as contamination by primary luminal cells (4, 6). Thus, in short-term culture deprived of the in vivo niche, myoepithelial cells (MEPs) have a tendency to undergo squamous metaplasia (10). Furthermore, in long-term culture, MEPs lose myodifferentiation permanently and fail to generate fully differentiated luminal cells (10–12). We here hypothesized that maintenance of the myoepithelial phenotype is critical for sustained progenitor cell activity, and that this requires continuous input from stroma. We describe a protocol that includes stromal feeders for serial subculture of MEPs with preserved phenotypic traits, progenitor cell activity, and no luminal contamination. Progenitor cell activity is revealed by clonal conversion into a luminal lineage upon feeder deprivation and correlates with in vivo breast morphogenesis upon transplantation to mice.

We show that the human breast contains two different progenitors: one residing within TDLUs, which is responsible for the typical luminal heterogeneity therein, and another in ducts, which has the potential to generate a homogeneous luminal lineage. We propose that this anatomy is the underlying cause of site-specific cancer susceptibility in the human breast.

Results

Luminal Heterogeneity in the Human Breast Is Region-Specific and Acquired. Simple keratins, such as K18 and K19, have been used successfully as readouts for stem cell activity in cultures of the human breast (4, 13–15). Among these, in particular, a heterogeneous staining for K19 in TDLUs and a homogeneous staining in interlobular ducts have been interpreted in favor of the existence of a breast stem cell hierarchy which is disrupted in breast cancer (5). Here, we tested this staining pattern with one

Significance

We have devised a culture system with conditions that allow primary breast myoepithelial cells (MEPs) to be passaged in a manner that sustains either nonmyodifferentiated or myodifferentiated cell populations without permitting contaminating luminal cells to grow. We show that progenitor activity and potency of MEPs to generate luminal cells in culture and in vivo rely on maintenance of myodifferentiation. Specific isolation and propagation of topographically distinct MEPs reveal the existence of multipotent progenitors in terminal duct lobular units. These findings have important implications for our understanding of the emergence of candidate luminal precursor cells to human breast cancer.

Author contributions: A.J.F., R.V., O.W.P., and L.R.-J. designed research; A.J.F., R.V., M.M., M.C.K., J.K., and L.R.-J. performed research; M.M. and J.K. contributed new reagents/analytic tools; A.J.F., R.V., M.M., O.W.P., and L.R.-J. analyzed data; and A.J.F., R.V., O.W.P., and L.R.-J. wrote the paper.

The authors declare no conflict of interest.

This article is a PNAS Direct Submission.

[1]A.J.F. and R.V. contributed equally to this work.

[2]To whom correspondence should be addressed. Email: lronnov-jessen@bio.ku.dk.

This article contains supporting information online at www.pnas.org/lookup/suppl/doi:10.1073/pnas.1714063114/-/DCSupplemental.

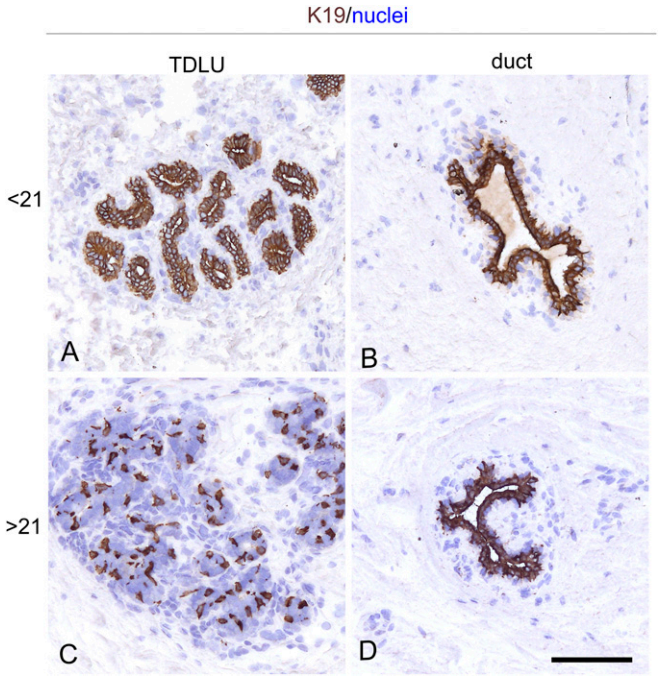

Fig. 1. Luminal heterogeneity is region-specific and acquired. Representative cryostat sections from a sample of reduction mammoplasties with prominent TDLUs, including 12 biopsies from women below the age of 21 y and 26 biopsies from women above the age of 21 y. All sections were stained for K19 by immunoperoxidase, and nuclei were counterstained with hematoxylin. Among younger women, almost all biopsies contained homogeneously $K19^+$ TDLUs (*A*); however, heterogeneity among TDLUs, defined as the presence of both prominent homogeneously $K19^+$ TDLUs and $K19^{+/-}$ TDLUs in the same section, was recorded primarily among women older than 21 y (*C*). (*B* and *D*) In both categories, ducts were homogeneously $K19^+$. (Scale bar: 50 μm.)

of the originally applied antibodies (BA16) on a sample of 38 normal biopsies. In all cases, interlobular ducts were homogeneously $K19^+$ (Fig. 1). Heterogeneity within TDLUs, here operationally defined as the presence of heterogeneous staining with K19 in more than one-third of the TDLUs in a given biopsy, increased with age (Fig. 1 and *SI Appendix*, Fig. S1). That the $K19^+$ cells indeed qualified as luminal cells was further supported by coexpression of K19 and the key luminal marker MUC1 (16, 17) (*SI Appendix*, Fig. S2), amounting to an average of $63 \pm 13\%$ of $K19^+$ cells with MUC1 expression in smears from three biopsies. A linear correlation between heterogeneity and age could, however, not be established (Spearman's rank correlation, $P = 0.07$), indicating that factors other than age per se may influence the pattern of K19 expression. One such factor is parity. In the present biopsy material, information about parity was not available, but among Danish women, less than 2% give birth before the age of 21 y (Statistics Denmark; www.Statbank.dk/FODP). Thus, we divided the material into two groups based on age below and above the age of 21 y. Heterogeneity was observed in one of 12 (8%) of the biopsies from women younger than 21 y of age and in 11 of 26 (42%) biopsies among women aged 21 to 59 y (Table 1). Aside from the one very heterogeneous biopsy among those from younger women, defined as an outlier based on the interquartile range method, the rest are significantly different from the group of older women (Mann–Whitney *U* test, $P < 0.05$). These data suggest that luminal heterogeneity is acquired specifically within the TDLUs. In light of our current understanding of luminal progenitors as being located downstream of myoepithelial stem cells, this raised the fundamental question of whether more than one myoepithelial progenitor cell compartment is responsible for sculpting the luminal lineage in the human breast, that is, whether ducts and lobules harbor different myoepithelial progenitor cells.

Control of Luminal Progenitor Formation from 2D Ultrapure MEPs. In previous work, we and others demonstrated that human MEPs under standard culture conditions rapidly lose the ability to differentiate into luminal epithelial cells (11, 12, 18). In the present work, to gauge for progenitor cell activity in TDLU- and duct-derived cells, respectively, we first developed a scalable, cell-based, serial passage subculture assay. Accordingly, we tested if a recently established 2D culture system for a highly uniform clonogenic ground state of intestinal stem cells (19, 20) could be modified to facilitate "ground state" human breast MEPs. Since freshly isolated human breast cells have been reported to contain about 8% multilineage progenitors (21) and some fluorescence-activated cell sorting (FACS) protocols for myoepithelial purification operate with contamination with primary luminal cells on the same order of magnitude (7), we first compared three established protocols (6, 22, 23) for their efficiency in recovering a pure myoepithelial population. As seen in Fig. 2*A*, irrespective of the

Table 1. List of biopsies used for heterogeneity scoring

Biopsy	Age, y	Heterogeneity score*	Frequency, %
P957	19	1/12	8
P985	19	2/15	13
P722/1	20	2/15	13
P648	13	0/14	0
W428/1	17	0/33	0
W432/1	18	4/31	13
W445/1	20	0/13	0
W466/3	18	3/11	27
F526	19	0/5	0
P944/2	18	0/6	0
P816	20	0/45	0
W430/1a	17	4/6	67
P967	34	4/8	50
P959/1	45	5/14	36
P954/1	39	2/11	18
P940/1	59	5/12	42
P931	44	4/8	50
P800	45	2/42	5
P737	44	0/20	0
P727/1	44	4/12	33
P832/1	32	3/26	12
P672/1	30	0/16	0
P837	23	7/14	50
P647/1	56	0/8	0
P670/3	42	7/18	39
P765	34	13/34	38
P819	45	0/14	0
P820	29	9/25	36
F498	46	11/47	23
P966	41	0/12	0
W430/2	59	7/35	20
W901	43	7/19	37
W1908/1	23	1/14	7
P653/1	40	2/18	11
P683/1	33	1/22	5
P941	27	13/24	54
F518s	24	0/26	0
W438	46	12/49	24

*Heterogeneity is scored as the number of K19 heterogeneous TDLUs/total number of TDLUs. Only biopsies with a frequency of 33% or higher were scored as positive.

FACS protocol applied, luminal contamination varied from 3 to 15%, which was considered too close to the hypothetical number of stem cells in the breast to represent a safe starting point. In an attempt to completely free the sorted population from luminal cells, we therefore tested the condition supportive of the intestinal ground state [i.e., a feeder of irradiated NIH 3T3 fibroblasts (19)] for its ability to select for myoepithelial plating and propagation when grown in a culture medium devised specifically for preservation of epithelial traits in culture [modified breastoid base medium with Y-27632, adenine, and serum replacement B27 (BBMYAB)] (22, 24), here termed Myo medium. While contaminating luminal cells plated and grew when seeded on plastic, this was not the case upon seeding on fibroblast feeders (Fig. 2*B*). By this protocol, ultrapure primary cultures of MEPs could be reproducibly generated from the $CD326^{low}/CD271^{high}$ gate of FACSs from a sample of 25 randomly selected biopsies.

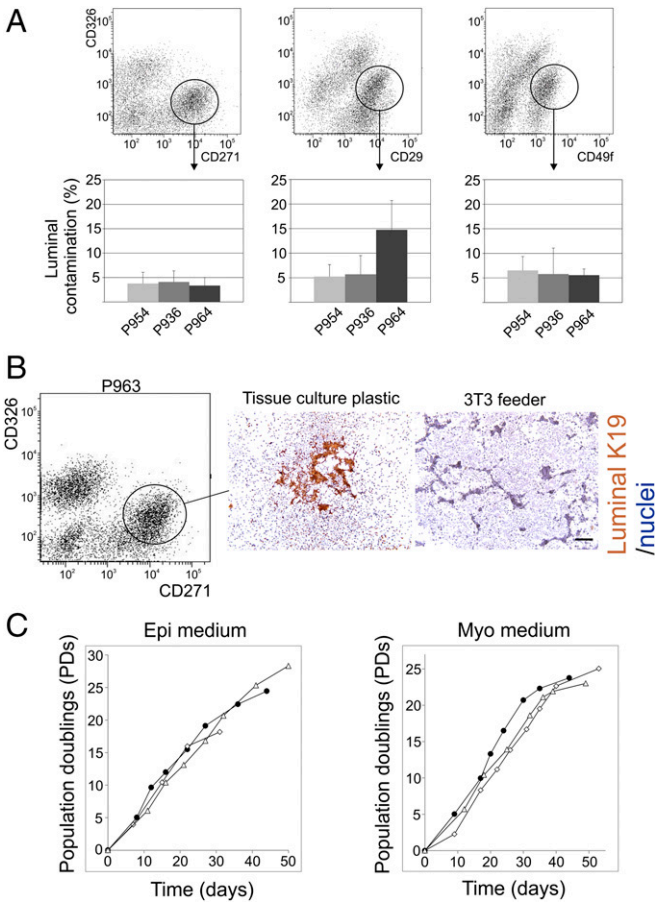

Fig. 2. Establishment of ultrapure 2D myoepithelial cultures as a source of luminal progenitors. (*A*, *Top*) FACS diagrams of MEPs from three independent reduction mammoplasties (P936, P954, and P964) sorted by three different protocols based on the application of a common antibody against luminal epithelial cells, CD326, in combination with one of the three myoepithelial markers: CD271 (*Left*), CD29 (*Middle*), and CD49f (*Right*). The circles indicate the approximate gates selected for sorting. (*A*, *Bottom*) Histograms based on quantification of luminal contamination as revealed by staining of K19 in smeared uncultured cells directly from FACS show contaminating luminal cells under all conditions, albeit at the lowest frequency with the CD271 protocol (error bars indicate SD). (*B*) MEPs from another biopsy (P963) sorted by the CD326/CD271 protocol (*Left*) and plated on either tissue culture plastic (*Middle*) or a 3T3 feeder (*Right*) and grown for 7 d in myoepithelial medium before staining. Luminal contamination, as revealed by the presence of islets of $K19^+$ cells, was strictly confined to tissue culture plastic. Nuclei are counterstained with hematoxylin. (Scale bar: 200 μm.) (*C*) MEPs from three independent reduction mammoplasties enriched by the CD326/CD271 protocol were propagated on 3T3 feeder cells under standard culture conditions (Epi medium) or a medium devised for maintenance of myoepithelial properties (Myo medium). Cells were counted and split consecutively at subconfluence. Accumulated population doublings were recorded as a function of time. Notably, there was no appreciable difference in longevity between the two culture protocols.

Once purified, it was essential to further expand MEPs exponentially in a scalable manner without spontaneous differentiation into luminal progenitors. We noted that the culture-induced irreversible loss of myoepithelial differentiation reported by us and others implicates the use of epidermal growth factor in the culture medium (10, 25, 26). Since MEPs in culture are either epithelium-like with little or no myodifferentiation or more mesenchymal-like cells with a full complement of myodifferentiation, we sought to examine both of these states of differentiation for their ability to serve in an assay for proper breast progenitor cell activity. For this purpose, we slightly modified a culture medium originally devised for long-term culture of human epithelial cells (FAD2) (27), here termed Epi medium, for comparison with the Myo medium. As seen in Fig. 2*C*, both media supported longevity, as revealed by growth for more than 25 population doublings. In the lower passages, the cultures could be split up to 1:40 and cultures could reach up to 10 passages, corresponding to approximately 2 mo in culture, before the cells senesced. Cultured normal human breast epithelial cells are known to encounter senescence barriers of which the first, stasis, is characterized by elevated levels of $CDKN2A/p16^{INK4A}$ (p16) (28). Here, up-regulation of p16 protein expression in passage 5 suggests that stasis is reached after 15–20 population doublings (*SI Appendix*, Fig. S3).

Using these conditions, we found that myoepithelial-derived cells in the presence of fibroblast feeders and irrespective of the applied culture medium completely refrained from luminal differentiation at any given time point during serial-passage subculture (Fig. 3 and *SI Appendix*, Fig. S4). The two media did, however, impact significantly on the differentiation repertoire. Both conditions supported expression of myoepithelial K14 and K5, as well as p63. However, whereas in Epi medium, the cells were nonmyodifferentiated myoepithelial cells (NMMEPs) exhibiting a relatively low expression of CD271, in Myo medium, the cells maintained critical differentiated traits of MEPs, including α-smooth muscle actin, vimentin, CD90, and CD271 (Fig. 3 and *SI Appendix*, Figs. S5 and S6). This was further confirmed by whole-transcript expression analysis and profiling (Fig. 4*A*). While NMMEPs exhibited high expression of transcripts related to keratinocyte and skin differentiation, MEPs highly expressed transcripts related to myodifferentiation (Fig. 4*A*). Switching the two culture media revealed that differentiation was unidirectional and that loss of myoepithelial differentiation was irreversible since MEPs became nonmyodifferentiated upon exposure to Epi medium, and upon switching to Myo medium, they remained epithelial, and myoepithelial characteristics were not gained.

Once verified as pure NMMEPs and MEPs, respectively, the cells' differentiation repertoire was further confirmed by in vivo orthotopic transplantation to NOG mice. MEPs developed into typical double-layered structures, including an outer layer of α-smooth muscle actin–positive MEPs, while the NMMEPs formed a lineage-restricted stratified epithelium without MEPs but with squamous characteristics, including K10 expression (Fig. 4*B*). Importantly, concomitant with their α-smooth muscle actin expression, MEPs performed in mice up to culture passage 4 without significant loss of morphogenic ability. This led us to conclude that we now are in possession of an ultrapure MEP serial-passage subculture protocol with preserved tissue-specific progenitor cell activity and, most importantly, that relevant breast progenitor cell activity relies on preserved myoepithelial differentiation.

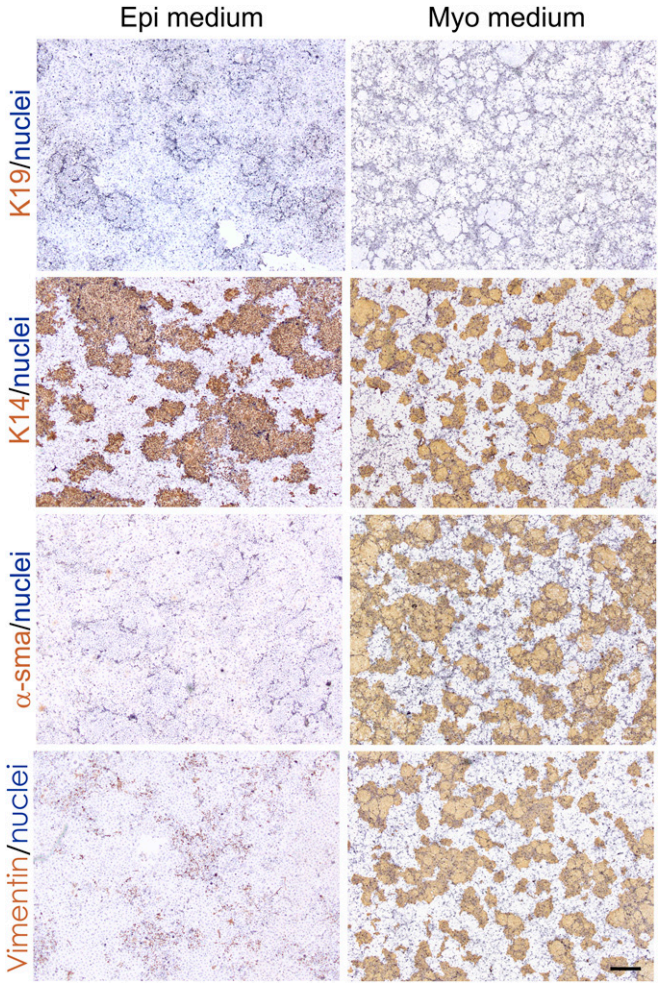

Fig. 3. Myoepithelial-derived cells in serial-passage subculture refrain from luminal conversion and exhibit an epithelial or myoepithelial phenotype depending on medium composition. Representative micrographs of myoepithelial-derived cells on 3T3 feeders grown in Epi medium (*Left*; $n = 14$ biopsies) or Myo medium (*Right*; $n = 20$ biopsies) stained with immunoperoxidase against K19, K14, α-smooth muscle actin (α-sma), and vimentin. Nuclei were counterstained with hematoxylin. Note that whereas all cells express K14, mesenchymal vimentin and α-sma are restricted to cells maintained under the myoepithelial culture protocol. (Scale bar: 500 μm.)

Gauging Luminal Progenitor Formation from Anatomically Well-Defined MEPs Reveals Region-Specific Multipotency in TDLUs. We next addressed whether the heterogeneous K19 staining in TDLUs and the homogeneous staining in ducts are the result of region-specific myoepithelial progenitor cell activity. We compared the potential of MEPs from the two locations with respect to generation of $K19^+$ luminal progenies in culture and in vivo. To induce luminal differentiation, we used an established protocol based on small-molecule TGF-β receptor inhibition (22, 29) combined with fibroblast feeder deprivation. First, we compared the frequency of MEPs with K19-forming capability in cultures from biopsies with a high content of TDLUs versus biopsies with a high content of ducts (up to sixfold higher, estimated as large ducts per total number of cells) (Fig. 5*A*). The $K19^+$ colony-forming ability was significantly lower in cultures derived from biopsies with a relatively high content of TDLUs compared with those with a high content of ducts (Fig. 5 *B* and *D* and *SI Appendix*, Fig. S7). Both sources of MEPs were able to generate structures upon transplantation into the mammary fat pad of NOG mice (Fig. 5*C*), and all transplantations resulted in structure formation (four of each). However, similar to the generation of $K19^+$ luminal progenies in culture, a lower number of $K19^+$ profiles out of the total number of profiles was consistently observed when MEPs were derived from TDLU-enriched biopsies compared with the number of profiles derived from duct-enriched biopsies (Fig. 5 *C* and *D*). The positive correlation observed between $K19^+$ colony-forming units in culture and $K19^+$ profiles in mice (Spearman's rank correlation coefficient: $\rho = 0.93$, $P < 0.005$; *SI Appendix*, Fig. S8) implied that the culture assay was useful as a surrogate readout of progenitor cell activity. The progenitors' ability to generate $K19^+$ colonies was estimated to a frequency of $4.3 \pm 3.7\%$, which is close to the frequencies of formation of mammospheres from aldefluor dehydrogenase-positive cells [~4% (30)] and daughter colony-forming cells from mammary repopulating units [$4.1 \pm 0.6\%$ (6)] reported by others. Also, luminal differentiation was not restricted to K19 only, as other key luminal markers were induced in culture as assessed by real-time (RT)-qPCR (*SI Appendix*, Fig. S9), and the luminal layer in MEP-derived structures in vivo further included expression of MUC1 and estrogen receptor-α (*SI Appendix*, Fig. S10).

If TDLUs and ducts indeed harbor different progenitor cell compartments as suggested by the above experiments, this should translate into a difference between MEPs derived from TDLUs and ducts within the same breast biopsy sample. To address this, we established MEP cultures from uncultured TDLU and duct organoids microcollected directly under a phase-contrast microscope (4), trypsinized into single cells, and sorted by FACS using the CD326/CD271 protocol (Fig. 6 *A* and *B*). These MEP cultures were further cloned for quantification of clonal capacity (Fig. 6*D*, *Left*), and the cloned cultures, in turn, were passaged to assess the K19 differentiating potential (Fig. 6 *C* and *D*, *Right*). While the clonal capacity of MEPs appeared similar in the two sites (Fig. 6*D*, *Left*), the K19 differentiation potential was significantly higher in duct-derived MEPs compared with those derived from TDLUs (Fig. 6*D*, *Right*; two-way ANOVA, $P < 0.05$). This suggests that the difference in K19 luminal differentiation is determined by a difference in progenitor cell potential between the two sites rather than by the number of progenitors per se.

With the aim of identifying markers useful for prospective isolation in bulk of duct versus TDLU MEPs, we screened a series of biopsies for surface and surrogate markers specific for duct MEPs. In all biopsies tested, we found that duct MEPs, as opposed to those from TDLUs, consistently stained for a small membrane glycoprotein, podoplanin (PDPN; reviewed in ref. 31) (Fig. 7*A*). These cells stained strongly with a candidate surrogate cytoskeletal marker, K17 (Fig. 7*A*). Based on this observation, we used a CD326/CD271/PDPN FACS-based protocol to prospectively isolate duct-derived MEPs (Fig. 7*B*). Smears of cells sorted by FACS and stained for K17 confirmed the specificity of this protocol for duct-derived $PDPN^{high}$ MEPs (Fig. 7*B*; $52 \pm 8\%$ $K17^+$ cells in the $PDPN^{high}$ preparation versus $6 \pm 3\%$ in the $PDPN^{low}$ preparation). Whereas plating of single cells in myoepithelial medium on feeders revealed no significant difference in colony-forming ability between the two sources of MEPs, further passaging of clones under differentiating conditions revealed that only duct-derived $PDPN^{high}$ clones were able to form homogeneous $K19^+$ colonies (Fig. 7*C*, *Right*). Whenever K19 was present in TDLU-derived clones, it was heterogeneously expressed, mostly with a scattered pattern of relatively small-sized colonies (Fig. 7*C*, *Left*). Collectively, these data are in strong favor of the existence of two functionally different stem cells in TDLUs and ducts of the normal human breast.

We finally addressed whether the heterogeneous and homogeneous expression of K19 observed in TDLU-derived and duct-derived MEP clones, respectively, might be a consequence of their progenitor cell potential (i.e., multipotency vs. bipotency). To that end, we transplanted enriched or cloned MEPs to the fat pad of NOG mice and stained by multicolor imaging for K19,

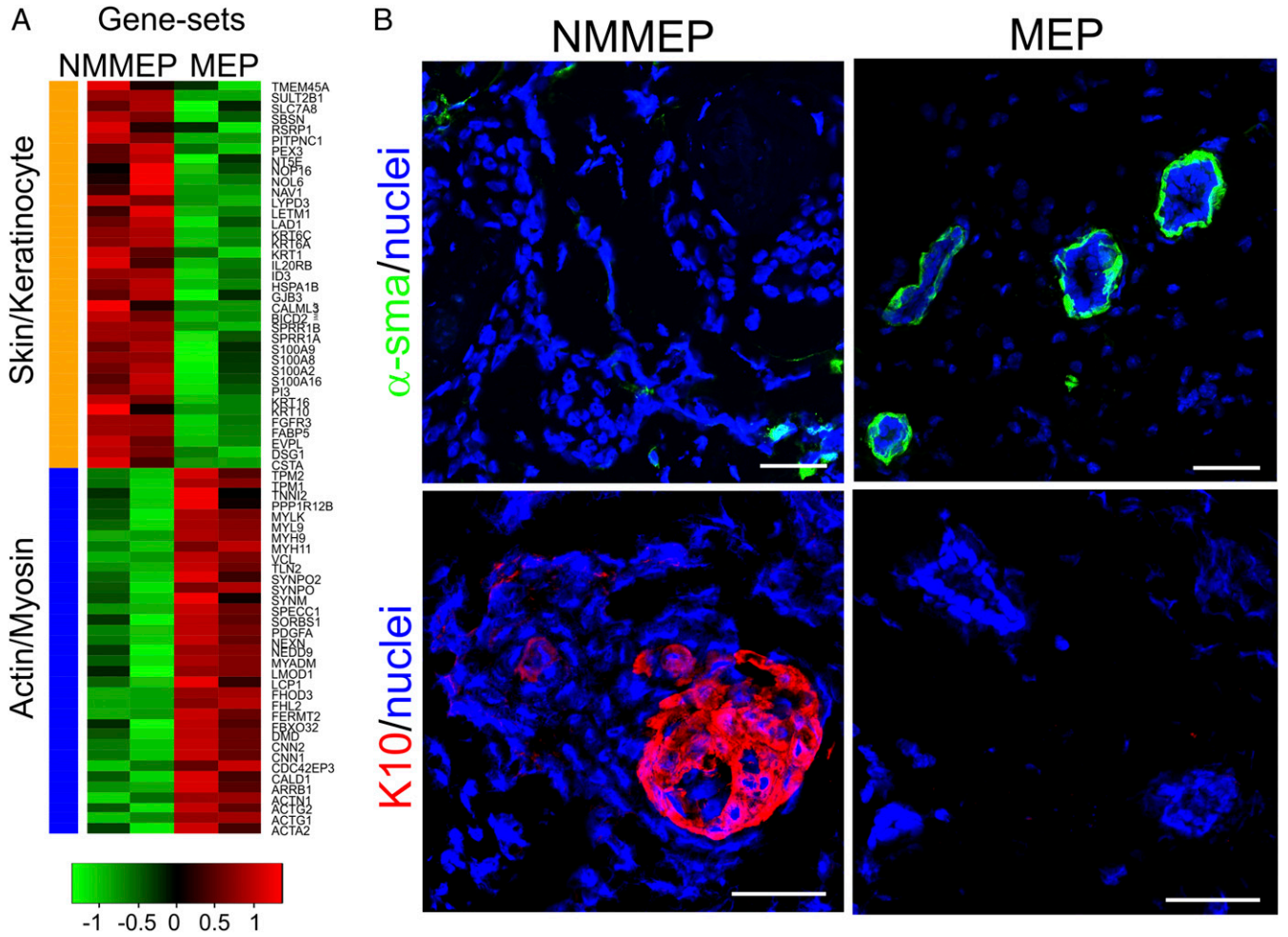

Fig. 4. Myodifferentiation of myoepithelial-derived cells depends on culture conditions. (*A*) Heat map of selected differentially expressed genes in NMMEPs or myodifferentiated MEPs. Whereas NMMEP transcripts are high in skin- and keratinocyte-associated transcripts (orange bar), MEP transcripts are high in actin- and myosin-associated transcripts (blue bar). Log_2-scaled expression values are presented for each gene, and the color key indicates the z-score ($n = 2$ biopsies). (*B*) Representative multicolor imaging of cryostat sections from xenografted NOG mice 8 wk after injection in the mammary fat pad of NMMEP-derived cells (*Left*; eight inoculations from three biopsies) or myoepithelial-derived cells (*Right*; 13 inoculations from six biopsies) stained against α-smooth muscle actin (α-sma; green) or K10 (red). Nuclei are counterstained with DAPI (blue). Note that whereas the myoepithelial-derived cells form relevant double-layered acini with a basal layer of α-sma$^+$ MEPs, the NMMEP-derived cells form skin-like keratin pearls are negative for α-sma and positive for K10. (Scale bars: 50 μm.)

α-smooth muscle actin, and K7, with the latter being a general marker of luminal breast epithelial cells. As a control, staining of TDLUs and ducts in sections of normal breast biopsies was included (Fig. 8). Luminal cells generated from MEPs derived from ducts stained uniformly with both K19 and K7 (Fig. 8*B*; 100 ± 0% K19$^+$/K7$^+$), while luminal cells from TDLUs that were otherwise K19$^-$ stained positive with K7 only (Fig. 8*A*; 100% K7$^+$, of which 7 ± 0.6% were K19$^+$/K7$^+$). Thus, the two sources of progenitor cells essentially recapitulated the TDLU and duct lineage generation observed in situ (Fig. 8 *C* and *D*). This indicates that the entire structure, including the MEPs derived from TDLUs, results from differentiation of multipotent progenitors as opposed to those from ducts, which derive from bipotent progenitors. Taken together, these results demonstrate a novel trajectory of cells in the anatomical region most susceptible to development of breast cancer.

Discussion

Several lines of evidence indicate that TDLUs are the predominant source of future breast cancers and that a high TDLU count is associated with genetic susceptibility variants and predicts higher breast cancer risk (32–35). The present work reveals that two functionally different progenitor cells reside within the myoepithelial lineage of the breast in the adult human: one associated with TDLUs and another localized to interlobular ducts. Furthermore, the TDLU-derived progenitors are responsible for a characteristic acquired heterogeneity within the luminal lineage, which is most frequently observed later in adulthood. However, a linear relationship between K19 heterogeneity and age cannot be established, perhaps reflecting that other factors, such as reproductive history, may influence the individual profile. In the present biopsy material, we do not have access to information about parity, for example, but the biopsies donated by women <21 y of age most likely represent nulliparous women. Indeed, parity is known to influence the molecular signature of human breast epithelial cells (36, 37). Whether parity-induced changes in cellular composition contribute to this altered profile remains to be elucidated. The results nevertheless indicate that TDLU-derived myoepithelial progenitor cells potentially contribute to the luminal lineage in the adult, and thus should be considered as candidate cells of origin of human breast cancer. The underlying mechanism for progenitor cell contribution remains to be established, and, at present, it

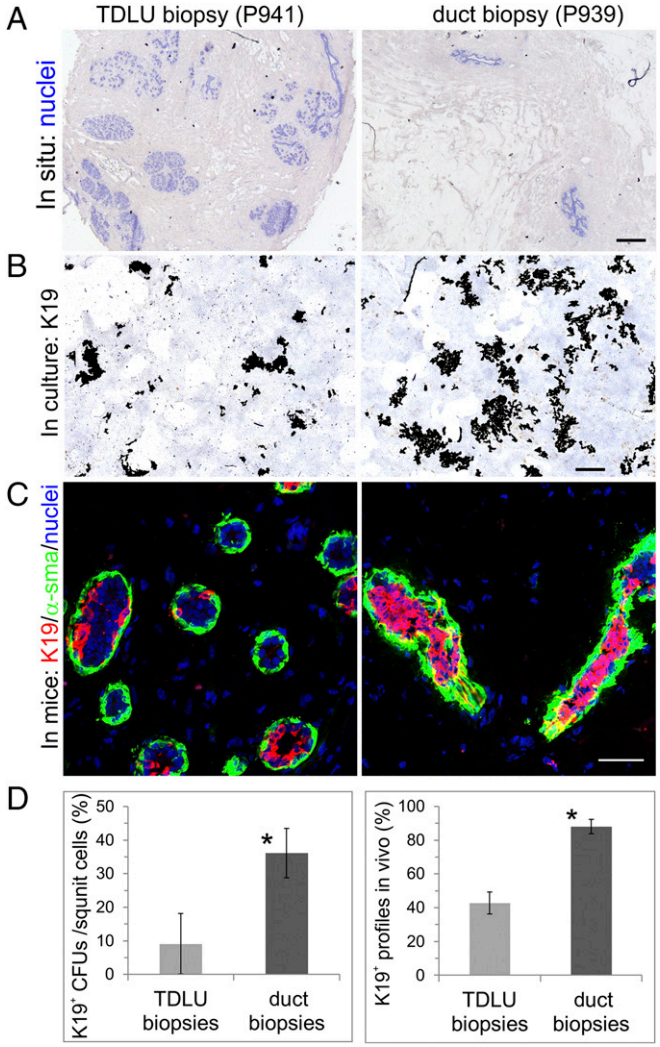

Fig. 5. TDLUs differ from ducts by their ability to generate K19$^+$ cells. (*A*) Low-magnification micrographs of cryostat sections of two independent biopsies with a high content of TDLUs (P941) and ducts (P939), respectively. Sections were stained with hematoxylin to highlight the histological differences (blue). (*B*) Low-magnification micrographs of generated luminal progenitor clones from MEP cultures derived from TDLU-enriched or duct-enriched biopsies stained with immunoperoxidase against K19 (brown) and nuclei (blue). The clones were digitized by image processing for area measurements. Note the higher number and larger clones in duct-derived cultures (*Right*) compared with the TDLU-derived cultures (*Left*). (*C*) Multicolor imaging of structures derived from MEP cultures from TDLU-enriched and duct-enriched biopsies transplanted to NOG mice in a humanized microenvironment with human breast fibroblasts and collagen I and Matrigel, and stained against K19 (red), α-smooth muscle actin (α-sma; green), and nuclei (blue). Whereas TDLU-derived morphogenesis was mainly heterogeneous with respect to K19 staining, the duct-derived profiles were generally homogeneously positive. (*D*) Histograms of quantification of luminal progenitor clones [K19$^+$ colony-forming units (CFUs) per square unit] in culture (*Left*) and luminal K19$^+$ structures in vivo (percentage of K19$^+$ profiles in vivo) in corresponding xenografts (*Right*) of MEPs from TDLU biopsies (gray bar, 11 inoculations from four biopsies) or duct biopsies (black bar, 11 inoculations from four biopsies). A significantly higher frequency of K19$^+$ clones and structures is generated from MEPs from duct biopsies [error bars indicate SDs; Student's *t* test: $*P = 0.0034$ (culture clones), $*P = 2.48\ E^{-5}$ (in vivo structures)]. (Scale bars: *A* and *B*, 500 μm; *C*, 50 μm.)

cannot be excluded that region-specific heterogeneity is due to an age-dependent impairment of differentiation capacity in bipotent progenitors. This would be consistent with previous findings that differentiation-defective multipotent progenitors accumulate with age (38–40). Also, future studies may reveal further complexity within the adult stem cell compartment in terms of subsets with a different repopulating activity and response to physiological stimuli, as demonstrated in the mouse gland (41). The findings presented here emphasize the myoepithelial lineage as an attractive target for the investigation of such mechanisms and of agents that promote or interfere with the formation of luminal breast cancer precursor cells.

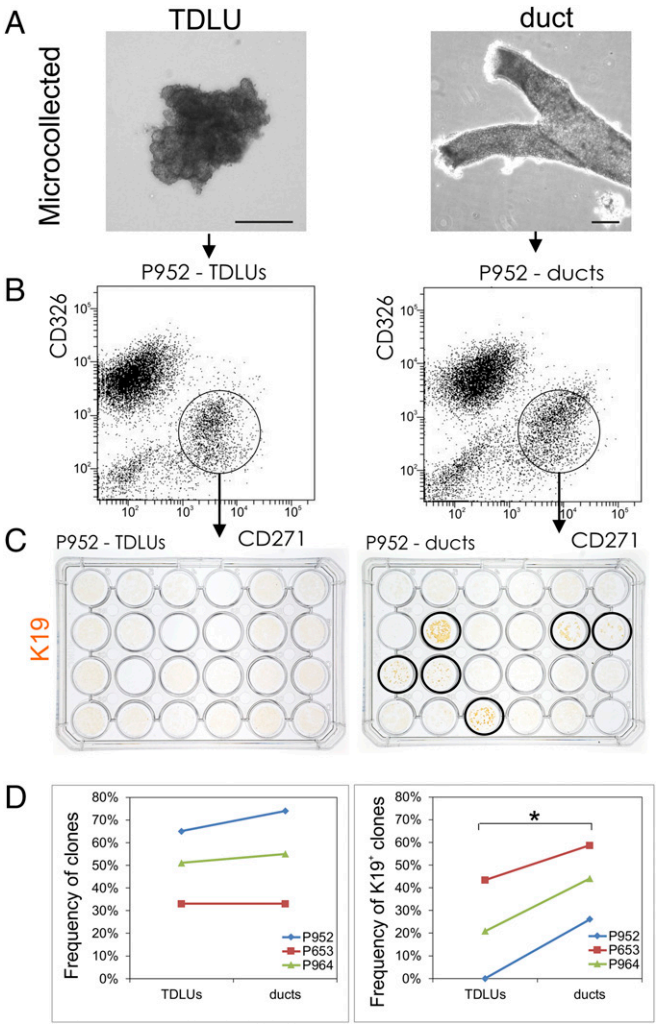

Fig. 6. TDLUs differ from ducts by K19 expression potential in MEP-derived clones. (*A*) Phase-contrast micrographs of microcollected TDLUs (*Left*) and ducts (*Right*). Only TDLUs without visible subtending ducts were selected for collection. (Scale bars: 100 μm.) (*B*) Representative FACS diagrams of trypsinized, microcollected TDLUs and ducts labeled with CD326 and CD271. The circles indicate the gating strategy, and the CD326/CD271 profiles of TDLUs and ducts are quite similar. (*C*) Second-passage clones in 24 well dishes stained with immunoperoxidase against K19 (brown) obtained from 96-well dishes with CD271^{high} single cells from TDLUs (*Left*) and ducts (*Right*), respectively. (*Right*) While all wells contain growing clones, in this particular biopsy, only CD271^{high}-derived clones from ducts are able to differentiate into keratin K19$^+$ descendants (circled wells). (*D*) Representative frequencies of colony-forming units from 96-well plates containing single CD271^{high} cells from three independent biopsies (*Left*; P952, P653, and P964) and their corresponding ability to convert into K19$^+$ descendants upon luminal differentiation (*Right*). TDLUs and ducts apparently exhibit an approximately similar capacity to form colonies (*Left*); however, within each biopsy, a significantly higher number of K19$^+$ clones are generated from ducts (*Right*) (two-way ANOVA test, $*P < 0.05$).

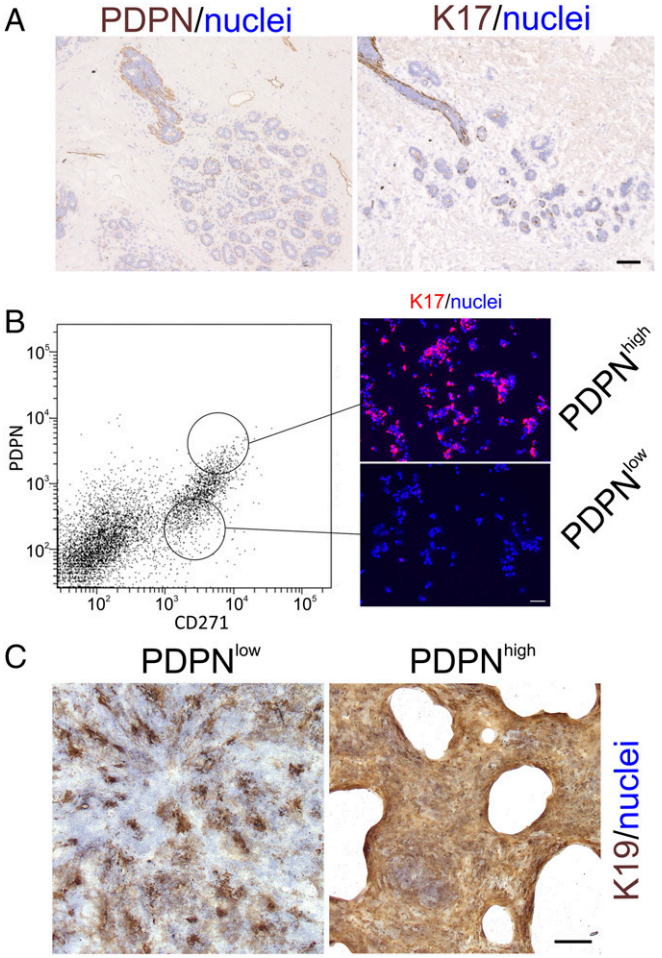

Fig. 7. Only duct-derived MEPs generate homogeneously $K19^+$ clones. (*A*) Representative immunoperoxidase stainings of cryostat sections of normal breast TDLUs with PDPN (*Left*) and K17 (*Right*). Nuclei are counterstained with hematoxylin (blue). A coordinate staining with the surface marker PDPN and the intracellular K17 is observed in ducts only. (*B*) FACS diagram of trypsinized breast tissue exposed to a CD326/CD271/PDPN protocol. (*Left*) Circles indicate the approximate gating strategy. (*Right*) Sorted $PDPN^{high}/CD271^{high}$ ($PDPN^{high}$) and $PDPN^{low}/CD271^{high}$ ($PDPN^{low}$) single cells were smeared and stained by fluorescence against K17 (red) and nuclei by DAPI (blue). Clearly, the $PDPN^{high}/CD271^{high}$ gate prospectively selects for duct-derived MEPs. (*C*) Low-magnification micrograph of representative single-cell clones from TDLU-derived ($PDPN^{low}$) and duct-derived ($PDPN^{high}$) differentiated MEP clones stained by immunoperoxidase against K19 (brown) and nuclei (blue). Homogeneous staining for K19 was confined to duct-derived MEP clones. (Scale bars: *A* and *B*, 50 μm; *C*, 500 μm.)

We have previously demonstrated the existence of luminal-derived human breast stem cells or progenitors based on the differentiation repertoire of cultured luminal epithelial cells and MEPs (11). This concurs nicely with the finding that human normal luminal progenitors are developmentally plastic and generate multilayered acinar structures when transplanted into female immunocompromised mice (14, 42). Subsequently, we further narrowed down the phenotype of candidate stem/progenitor cells in the human breast to a suprabasal $K14^+/K19^+$ cell with a preferential ductal localization (4, 13). Here, we identify progenitor activity by the appearance of $K19^+$ clones on a $K14^+$ background. We therefore suspect that the previously described $K14^+/K19^+$ suprabasal progenitors are very closely related to at least the ductal myoepithelial-derived progenitors in the present study. Indeed, the K14/K19 readout currently seems to be the most operational surrogate marker for progenitor cells in culture within the context of the human breast (39, 43).

The TDLU is an anatomical structure which is permanently present, particularly in the human breast. Even in the nulliparous state, the human breast is more developmentally advanced than that of the adult mouse mammary gland (reviewed in ref. 44). However, the human TDLU does not remain static throughout a lifetime. Both in terms of size and molecular markers, it changes with endocrinological and reproductive history (45). Most of the cellular turnover responsible for such hormone-induced TDLU remodeling takes place within the luminal epithelial lineage (4). Whether or not bona fide stem cells play a role has remained an open question. This is of interest because, in most tissues, stem cells are believed to stay long enough within the tissue to sustain and accumulate the mutations necessary for cellular transformation (46). Indeed, in the human breast, stem cells have been compellingly demonstrated using a transplantation protocol based on severely immunocompromised mice (6, 7). As in the mouse mammary gland, the human breast stem cells are embedded within the myoepithelial lineage (8). This implies that a potential contribution of human breast stem cells to human breast cancer should be traceable to the myoepithelial lineage. Surprisingly, in mice, although cellular turnover at homeostasis seems to be strictly maintained by self-duplication within the lineages, disturbance (e.g., upon single-cell transplantation or activation of oncogenic pathways) leads to destabilization of the

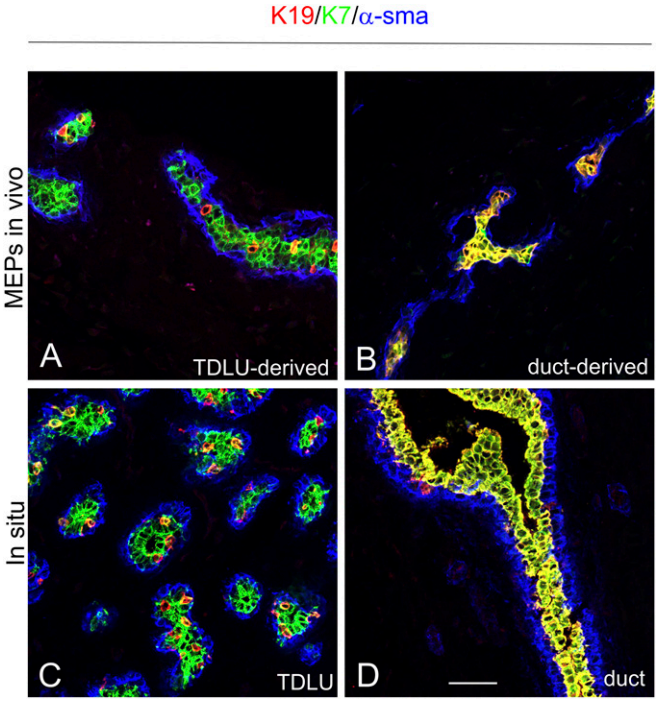

Fig. 8. TDLU- and duct-derived progenitors are multipotent and bipotent, respectively. Multicolor imaging of cryostat sections from microcollected enriched TDLU-derived (*A*) and single-cell–cloned duct-derived (*B*) MEPs inoculated into the fat pad of NOG mice (MEPs in vivo) compared with TDLUs (*C*) and ducts of human breast tissue (in situ) (*D*) stained with K19 (red), K7 (green), and α-smooth muscle actin (α-sma; blue). Whereas single-cell–cloned duct-derived progenitors consistently exhibited only two cell types [i.e., $K7^+/K19^+$ luminal cells (yellow), $\alpha\text{-sma}^+$ MEPs (blue); structures formed from one of three clones, three inoculations in two mice], the TDLU-derived progenitors, as an indication of multipotency, additionally gave rise to heterogeneous profiles consisting of two luminal cell populations, of which one expressed K7 only, as well as a population of $\alpha\text{-sma}^+$ MEPs (blue; microcollected TDLUs, four inoculations in four mice). (Scale bar: 50 μm.)

myoepithelial phenotype and conversion into luminal precursor cells, and eventually luminal cancer (3, 47, 48). Due to the presence of permanently active TDLUs in the human gland, disturbances of tissue homoeostasis are likely to be more frequent on a lifetime scale than in mice. Consequently, TDLU-resident myoepithelial stem cells are likely to contribute progenitors to the luminal lineage more often in humans. Intriguingly, microdissection with the purpose of isolating morphologically distinct regions of apparently normal breast tissue adjacent to breast cancer has revealed a "field effect" in which some of the genetic aberrations found in the invasive cancer were also present in neighboring normal TDLUs (49, 50). Importantly, Deng et al. (49) found that TDLUs more distant to the tumor were quite normal. It was concluded that loss of heterozygosity (LOH) in certain TDLUs confers focal increased risk of breast cancer, which may impact on the risk of tumor recurrence. The finding of LOH in human TDLUs is in strong favor of a clonal origin of this structure. Nevertheless, our data are in favor of the idea that even though the myoepithelial lineage, presumably in fetal life, arises clonally in common antecedents (51), in the adult, luminal progenitors within TDLUs are fueled in a facultative manner by progenitor cells which have undergone some alteration in differentiation repertoire with adulthood (reviewed in ref. 52). Whether other factors, such as reproductive history or use of oral contraceptives, additionally influence this differentiation pattern is currently unknown.

We and others have previously argued that although tumor-derived MEPs do not exhibit gross genomic alterations, they are phenotypically severely abnormal (53, 54). Here, we find luminal progenies in TDLUs of adults of older age. This finding may concur with previous observations on TDLUs from BRCA carriers in which LOH is not necessarily the result of very early aberrations but is acquired later (55). Thus, genetic alterations vary from one clone to another in the tissue and extend beyond a single TDLU, suggesting an acquired instability within the entire area of the breast (55).

The exact mechanism by which aberrant TDLUs predispose to breast cancer remains unknown. However, the sheer number of TDLUs and the number of acini per TDLU have been associated with the presence of known cancer genetic susceptibility variants (33). Also, signaling pathways controlling the cellular composition of the human breast have been explored for cancer risk assessment and prevention (56, 57). For example, differentiated MEPs have been shown to be tumor-suppressive (58), the activity of stem cell-related signaling in $P27^{+}$ progenitors correlates with the risk of developing breast cancer (56), and BMP2 levels influence the conversion of preneoplastic stem cells into luminal breast cancer (57).

The paradigm identified here for the topographical generation of luminal progenitors from myoepithelial progenitors within human breast TDLUs may impact on the general concept of cell of origin in human breast cancer. Thus, the cell of origin determines the phenotype of a derived tumor by both its initial chromatin state and its transcriptional priming, which eventually translate into tumor aggressiveness (59). We speculate that in targeting stem cells or progenitors in the human breast with respect to modeling tumor evolution, it is indispensable to take into account specifically the TDLU. If this is proven correct, it may facilitate understanding of the functional diversity of human breast tumors and further the development of precision medicine.

Materials and Methods

Tissue. Normal breast biopsies were collected from healthy women undergoing reduction mammoplasty for cosmetic reasons. Donors were informed before surgery and agreed by written consent to donate tissue. The use of human material has been reviewed by the Regional Scientific Ethical Committees (Region Hovedstaden) and approved with reference to H-2-2011-052. The only available information about the donors is their age at the time of surgery. Material from some of the biopsies had been included in previous studies. Normal breast tissue was prepared, and epithelial organoids and fibroblasts were isolated as previously described (60). The epithelial organoids were either used directly or frozen in liquid nitrogen for later use (90% FBS/10% dimethyl sulfoxide; Sigma–Aldrich).

FACS. For analysis of epithelial cell composition and sorting of single cells, epithelial organoids or microcollected TDLUs and ducts were trypsinized for 5–10 min in 0.25% trypsin and 1 mM EDTA solution under rotation at 37 °C. Trypsination was stopped by addition of FBS and followed by filtration through 100-μm mesh (Streno). Single cells were suspended in Hepes buffer supplemented with 0.5% BSA (fraction V; Sigma–Aldrich) and 2 mM EDTA (Merck), pH 7.5. To separate MEPs from luminal cells and optimize purification of MEPs, the suspended cells were incubated for 45 min at 4 °C in the presence of fluorochrome-conjugated monoclonal antibodies according to three different protocols: EpCAM/CD326-AF488 (9C4, 1:50; BioLegend) or CD326-BV421 (EBA-1, 1:50; BD Biosciences) in combination with p75 neurotrophin receptor $p75^{(NTR)}$/CD271-allophycocyanin (APC) (ME20.4, 1:50; Cedarlane Laboratories), EpCAM/CD326-AF647 (9C4, 1:50; BioLegend) in combination with CD29-AF488 (TS2/16, 1:50; BioLegend), or EpCAM/CD326-AF647 in combination with CD49f-FITC (GoH3, 1:50; BD Biosciences) (*SI Appendix*, Table S1). The former protocol isolating $CD326^{low}$/$CD271^{high}$ cells was employed in subsequent experiments.

Cell Culture. For establishment and serial passage of ultrapure myodifferentiated MEPs, sorted primary MEPs (n = 30 biopsies) were plated on a confluent layer of irradiated NIH 3T3 feeder cells (20 Gy, 4–8 × 10^3 cells per square centimeter) in basic breastoid medium without Hepes (BBMYAB, modified from ref. 26), here called Myo medium, and NMMEPs were propagated in FAD2 medium (modified from refs. 27, 61), here called Epi medium. Details are provided in *SI Appendix*.

Cell Propagation, Differentiation, and Clonal Colony Formation. Growth curves were established from three different biopsies as parallel cultures in Epi or Myo medium and plotted as population doublings versus time. For each passage, 2,000–20,000 cells per square centimeter were plated on fibroblast feeders and counted manually with a counter chamber at 80–90% confluence. Population doublings were calculated as $n = 3.32(\log UCY - \log I) + X$, where n is population doubling, UCY is cell yield, I is inoculum number, and X is population doubling of inoculum.

Luminal differentiation was induced as detailed in *SI Appendix*.

Microcollected ducts and TDLUs (n = 4 biopsies) were manually separated under an inverted phase-contrast microscope as previously described (4). Collected organoids were prepared for sorting as described in *SI Appendix*.

For generation of single-cell clones (either from microcollected TDLUs and ducts or from $PDPN^{high}$ and $PDPN^{low}$ cells), cells were sorted with the automated cell deposition unit (ACDU) unit of FACSAria/FACSFusion into a 96-well plate (five cells per well) preplated with irradiated NIH 3T3 feeders in the presence of myoepithelial medium and monitored for the establishment of epithelial islets for 2–3 wk. Wells with the appearance of two islets or more were discarded. When islets reached a sufficient size for further propagation, cells were trypsinized and plated in 24-well plates under culture conditions that induce luminal differentiation. In some cases, a portion of the MEPs were plated onto new feeders for further expansion before in vivo transplantation.

In Vivo Transplantation. Animal experiments were performed with permission from the Animal Experiments Inspectorate (J.nr. 2012-15-2934-00571) and performed as described in *SI Appendix*.

RNA Isolation, RT-qPCR, and RNA-Sequencing Analysis. For RT-qPCR, $CD326^{low}$/$CD271^{high}$ cells were cultured in Myo medium on feeders for 9 d and passaged to collagen-coated cultures with MEGM and RepSox without feeders to generate luminal progenitors. After 13 d, the cells were sorted by FACS upon incubation with CD117 to isolate generated $CD117^{high}$ $K19^{+}$ progenitors for comparison with MEPs, and upon RNA extraction, RT-qPCR was performed with primers listed in *SI Appendix*, Table S2. A list of significantly differentially expressed genes was established based on the noise sequencing (NOIseq) method.

Immunohistochemistry and Cytochemistry. Cryostat sections, smears of cells sorted by FACS, and monolayer cultures were prepared and stained by immunoperoxidase or immunofluorescence essentially as previously described (4, 10, 62), and antibodies are listed in *SI Appendix*, Table S1.

Western Blotting. Whole-cell lysates of MEPs were prepared in passages 2, 5, and 7, and blotting was performed as described in *SI Appendix*.

Statistics. All statistical analyses were performed by the statistical computing program R (version 3.3.2). The Mann–Whitney *U* test was applied for comparison of two nonparametric groups, an interquartile range method was used for identifying outliers, a two-way ANOVA analysis or Student's *t* test was used for testing difference between two groups, and a Spearman's rank correlation test was used for determination of significant correlation between two variables.

All other materials and methods can be found in *SI Appendix, SI Materials and Methods*.

ACKNOWLEDGMENTS. We thank Tove Marianne Lund, Lena Kristensen, and Charlotte Petersen for expert technical assistance. We thank Dr. Benedikte Thuesen (Capio CFR) and the donors for providing the normal breast biopsy material, and Vera Timmermans Wielenga (Pathology Department, Rigshospitalet) for confirming the normalcy of the tissue. The Core Facility for Integrated Microscopy (Faculty of Health and Medical Sciences, University of Copenhagen) is acknowledged for confocal microscope accessibility. This work was supported by the Novo Nordisk Fonden and Danish Research Council Grant 10-092798 (to DanStem), the Kirsten and Freddy Johansens Fond (O.W.P.), the Familien Erichsens Mindefond and Vera og Carl Johan Michaelsens Legat (J.K.), the Anita og Tage Therkelsens Fond (R.V.), and the Harboefonden and Else og Mogens Wedell-Wedellsborgs Fond and Danish Cancer Society Grant R146-A9257 (to L.R.-J.).

1. Tabár L, et al. (2014) A proposal to unify the classification of breast and prostate cancers based on the anatomic site of cancer origin and on long-term patient outcome. *Breast Cancer (Auckl)* 8:15–38.
2. Hovey RC, Trott JF, Vonderhaar BK (2002) Establishing a framework for the functional mammary gland: From endocrinology to morphology. *J Mammary Gland Biol Neoplasia* 7:17–38.
3. Carroll JS, Hickey TE, Tarulli GA, Williams M, Tilley WD (2017) Deciphering the divergent roles of progestogens in breast cancer. *Nat Rev Cancer* 17:54–64.
4. Villadsen R, et al. (2007) Evidence for a stem cell hierarchy in the adult human breast. *J Cell Biol* 177:87–101.
5. Bartek J, Taylor-Papadimitriou J, Miller N, Millis R (1985) Patterns of expression of keratin 19 as detected with monoclonal antibodies in human breast tissues and tumours. *Int J Cancer* 36:299–306.
6. Eirew P, et al. (2008) A method for quantifying normal human mammary epithelial stem cells with *in vivo* regenerative ability. *Nat Med* 14:1384–1389.
7. Lim E, et al.; kConFab (2009) Aberrant luminal progenitors as the candidate target population for basal tumor development in *BRCA1* mutation carriers. *Nat Med* 15: 907–913.
8. Prater MD, et al. (2014) Mammary stem cells have myoepithelial cell properties. *Nat Cell Biol* 16:942–950, 1–7.
9. Okkenhaug K, Roychoudhuri R (2015) Oncogenic PI3Kα promotes multipotency in breast epithelial cells. *Sci Signal* 8:pe3.
10. Petersen OW, van Deurs B (1988) Growth factor control of myoepithelial-cell differentiation in cultures of human mammary gland. *Differentiation* 39:197–215.
11. Péchoux C, Gudjonsson T, Rønnov-Jessen L, Bissell MJ, Petersen OW (1999) Human mammary luminal epithelial cells contain progenitors to myoepithelial cells. *Dev Biol* 206:88–99.
12. Keller PJ, et al. (2010) Mapping the cellular and molecular heterogeneity of normal and malignant breast tissues and cultured cell lines. *Breast Cancer Res* 12:R87.
13. Gudjonsson T, et al. (2002) Isolation, immortalization, and characterization of a human breast epithelial cell line with stem cell properties. *Genes Dev* 16:693–706.
14. Keller PJ, et al. (2012) Defining the cellular precursors to human breast cancer. *Proc Natl Acad Sci USA* 109:2772–2777.
15. Arendt LM, et al. (2014) Anatomical localization of progenitor cells in human breast tissue reveals enrichment of uncommitted cells within immature lobules. *Breast Cancer Res* 16:453–468.
16. Hilkens J, et al. (1984) Monoclonal antibodies against human milk-fat globule membranes detecting differentiation antigens of the mammary gland and its tumors. *Int J Cancer* 34:197–206.
17. Petersen OW, van Deurs B (1986) Characterization of epithelial membrane antigen expression in human mammary epithelium by ultrastructural immunoperoxidase cytochemistry. *J Histochem Cytochem* 34:801–809.
18. Taylor-Papadimitriou J, et al. (1989) Keratin expression in human mammary epithelial cells cultured from normal and malignant tissue: Relation to in vivo phenotypes and influence of medium. *J Cell Sci* 94:403–413.
19. Wang X, et al. (2015) Cloning and variation of ground state intestinal stem cells. *Nature* 522:173–178.
20. Shimokawa M, Sato T (2015) Back to 2D culture for ground state of intestinal stem cells. *Cell Stem Cell* 17:5–7.
21. Dontu G, et al. (2003) In vitro propagation and transcriptional profiling of human mammary stem/progenitor cells. *Genes Dev* 17:1253–1270.
22. Fridriksdottir AJ, et al. (2015) Propagation of oestrogen receptor-positive and oestrogen-responsive normal human breast cells in culture. *Nat Commun* 6: 8786–8797.
23. Shackleton M, et al. (2006) Generation of a functional mammary gland from a single stem cell. *Nature* 439:84–88.
24. Morsing M, et al. (2016) Evidence of two distinct functionally specialized fibroblast lineages in breast stroma. *Breast Cancer Res* 18:108–117.
25. Deugnier MA, et al. (2002) EGF controls the in vivo developmental potential of a mammary epithelial cell line possessing progenitor properties. *J Cell Biol* 159:453–463.
26. Pasic L, et al. (2011) Sustained activation of the HER1-ERK1/2-RSK signaling pathway controls myoepithelial cell fate in human mammary tissue. *Genes Dev* 25:1641–1653.
27. Liu X, et al. (2012) ROCK inhibitor and feeder cells induce the conditional reprogramming of epithelial cells. *Am J Pathol* 180:599–607.
28. Garbe JC, et al. (2014) Immortalization of normal human mammary epithelial cells in two steps by direct targeting of senescence barriers does not require gross genomic alterations. *Cell Cycle* 13:3423–3435.
29. Bruna A, et al. (2012) TGFβ induces the formation of tumour-initiating cells in claudin^{low} breast cancer. *Nat Commun* 3:1055.
30. Ginestier C, et al. (2007) ALDH1 is a marker of normal and malignant human mammary stem cells and a predictor of poor clinical outcome. *Cell Stem Cell* 1:555–567.
31. Ugorski M, Dziegiel P, Suchanski J (2016) Podoplanin–A small glycoprotein with many faces. *Am J Cancer Res* 6:370–386.
32. Cardiff RD, et al. (2002) Contributions of mouse biology to breast cancer research. *Comp Med* 52:12–31.
33. Bodelon C, et al. (2017) Association between breast cancer genetic susceptibility variants and terminal duct lobular unit involution of the breast. *Int J Cancer* 140: 825–832.
34. Oh H, et al. (2016) Relation of serum estrogen metabolites with terminal duct lobular unit involution among women undergoing diagnostic image-guided breast biopsy. *Horm Cancer* 7:305–315.
35. Figueroa JD, et al. (2016) Standardized measures of lobular involution and subsequent breast cancer risk among women with benign breast disease: A nested case-control study. *Breast Cancer Res Treat* 159:163–172.
36. Peri S, et al. (2012) Defining the genomic signature of the parous breast. *BMC Med Genomics* 5:46.
37. Rotunno M, et al. (2014) Parity-related molecular signatures and breast cancer subtypes by estrogen receptor status. *Breast Cancer Res* 16:R74.
38. Garbe JC, et al. (2012) Accumulation of multipotent progenitors with a basal differentiation bias during aging of human mammary epithelia. *Cancer Res* 72:3687–3701.
39. Pelissier FA, et al. (2014) Age-related dysfunction in mechanotransduction impairs differentiation of human mammary epithelial progenitors. *Cell Rep* 7:1926–1939.
40. Lee JK, et al. (2015) Age and the means of bypassing stasis influence the intrinsic subtype of immortalized human mammary epithelial cells. *Front Cell Dev Biol* 3:13.
41. Fu NY, et al. (2017) Identification of quiescent and spatially restricted mammary stem cells that are hormone responsive. *Nat Cell Biol* 19:164–176.
42. Shehata M, et al. (2012) Phenotypic and functional characterisation of the luminal cell hierarchy of the mammary gland. *Breast Cancer Res* 14:R134.
43. Britschgi A, et al. (2017) The Hippo kinases LATS1 and 2 control human breast cell fate via crosstalk with ERα. *Nature* 541:541–545.
44. Rønnov-Jessen L, Petersen OW, Bissell MJ (1996) Cellular changes involved in conversion of normal to malignant breast: Importance of the stromal reaction. *Physiol Rev* 76:69–125.
45. Russo J, Hu Y-F, Yang X, Russo IH (2000) Developmental, cellular, and molecular basis of human breast cancer. *J Natl Cancer Inst Monogr* 27:17–37.
46. Owens DM, Watt FM (2003) Contribution of stem cells and differentiated cells to epidermal tumours. *Nat Rev Cancer* 3:444–451.
47. Koren S, et al. (2015) PIK3CA(H1047R) induces multipotency and multi-lineage mammary tumours. *Nature* 525:114–118.
48. Van Keymeulen A, et al. (2015) Reactivation of multipotency by oncogenic PIK3CA induces breast tumour heterogeneity. *Nature* 525:119–123.
49. Deng G, Lu Y, Zlotnikov G, Thor AD, Smith HS (1996) Loss of heterozygosity in normal tissue adjacent to breast carcinomas. *Science* 274:2057–2059.
50. Lakhani SR, et al. (1999) Genetic alterations in 'normal' luminal and myoepithelial cells of the breast. *J Pathol* 189:496–503.
51. George AL, Smith GH (2016) Mammary epithelial cell lineage analysis via the Lyon's hypothesis. *Int J Stem Cell Res Ther* 3:1–8.
52. Petersen OW, Polyak K (2010) Stem cells in the human breast. *Cold Spring Harb Perspect Biol* 2:a003160.
53. Gudjonsson T, et al. (2002) Normal and tumor-derived myoepithelial cells differ in their ability to interact with luminal breast epithelial cells for polarity and basement membrane deposition. *J Cell Sci* 115:39–50.
54. Allinen M, et al. (2004) Molecular characterization of the tumor microenvironment in breast cancer. *Cancer Cell* 6:17–32.
55. Clarke CL, et al. (2006) Mapping loss of heterozygosity in normal human breast cells from BRCA1/2 carriers. *Br J Cancer* 95:515–519.
56. Choudhury S, et al. (2013) Molecular profiling of human mammary gland links breast cancer risk to a p27(+) cell population with progenitor characteristics. *Cell Stem Cell* 13:117–130.
57. Chapellier M, et al. (2015) Disequilibrium of BMP2 levels in the breast stem cell niche launches epithelial transformation by overamplifying BMPR1B cell response. *Stem Cell Rep* 4:239–254.
58. Barsky SH, Karlin NJ (2006) Mechanisms of disease: Breast tumor pathogenesis and the role of the myoepithelial cell. *Nat Clin Pract Oncol* 3:138–151.

59. Latil M, et al. (2017) Cell-type specific chromatin states differentially prime squamous cell carcinoma tumor-initiating cells for epithelial to mesenchymal transition. *Cell Stem Cell* 20:191–204.e5.
60. Rønnov-Jessen L, Petersen OW (1993) Induction of α-smooth muscle actin by transforming growth factor-β 1 in quiescent human breast gland fibroblasts. Implications for myofibroblast generation in breast neoplasia. *Lab Invest* 68:696–707.
61. Tan DWM, et al. (2013) Single-cell gene expression profiling reveals functional heterogeneity of undifferentiated human epidermal cells. *Development* 140: 1433–1444.
62. Rønnov-Jessen L, Celis JE, Van Deurs B, Petersen OW (1992) A fibroblast-associated antigen: Characterization in fibroblasts and immunoreactivity in smooth muscle differentiated stromal cells. *J Histochem Cytochem* 40:475–486.